



# The propofol-induced mitochondrial damage in fetal rat hippocampal neurons via the AMPK/P53 signaling pathway

Fei Xiao<sup>1^#</sup>, Yi Qin<sup>1^#</sup>, Jing Chen<sup>1^#</sup>, Chunlai Li<sup>1</sup>, Yinying Qin<sup>1</sup>, Yi Wei<sup>1</sup>, Yubo Xie<sup>1,2^A</sup>

<sup>1</sup>Department of Anesthesiology, The First Affiliated Hospital of Guangxi Medical University, Nanning, China; <sup>2</sup>Guangxi Key Laboratory of Enhanced Recovery after Surgery for Gastrointestinal Cancer, The First Affiliated Hospital of Guangxi Medical University, Nanning, China

**Contributions:** (I) Conception and design: Y Xie, Y Wei, F Xiao; (II) Administrative support: Y Xie; (III) Provision of study materials or patients: F Xiao, Yi Qin; (IV) Collection and assembly of data: J Chen, C Li; (V) Data analysis and interpretation: F Xiao, Yinying Qin; (VI) Manuscript writing: All authors; (VII) Final approval of manuscript: All authors.

<sup>#</sup>These authors contributed equally to this work.

**Correspondence to:** Yubo Xie; Yi Wei. Department of Anesthesiology, The First Affiliated Hospital of Guangxi Medical University, Nanning, China. Email: xybdoctor@163.com; yi45789@sina.com.

**Background:** Propofol is a commonly used general anesthetic that may cause neuronal damage, especially in infants and young children. Mitochondria play an essential role in cellular metabolism and signal transduction. Propofol may cause neurotoxicity by inhibiting mitochondrial function, but the mechanism by which this occurs remains unclear.

**Methods:** First, the primary rat hippocampal neurons were cultured for 7 days *in vitro*. The neurons were incubated with propofol at different times or different concentrations, and then the adenosine triphosphate (ATP), reactive oxygen species (ROS), mitochondrial membrane potential, and apoptosis-related proteins were analyzed. Based on the results of the 1st phase, the neurons were then incubated with propofol (100  $\mu$ M) or corresponding reagents, including 5-aminoimidazole-4-carboxamide ribonucleotide, tenovin-1, and pifithrin- $\alpha$ . Subsequently, the ATP, ROS, mitochondrial membrane potential, phospho-adenosine 5'-monophosphate-activated protein kinase (p-AMPK), protein 53 (p53), and related apoptosis proteins were analyzed.

**Results:** Higher propofol concentrations or longer incubation times were associated with more pronounced decreases in ATP, B-cell lymphoma 2 (Bcl-2), and mitochondrial membrane potential, and more pronounced increases in ROS, BCL2-associated X (Bax), Cytochrome C (CytC), and cleaved caspase-9. Additionally, after incubation with propofol (100  $\mu$ M), neuronal Bcl-2, p-AMPK, ATP, and mitochondrial membrane potential were downregulated, and ROS, p53, CytC, Bax, cleaved caspase-3, and cleaved caspase-9 were upregulated. AMPK activators or p53 inhibitors reversed the above-mentioned changes.

**Conclusions:** Propofol (100  $\mu$ M)-induced mitochondrial damage in fetal rat hippocampal neurons may be mediated by the AMPK/p53 signaling pathway. Propofol (100  $\mu$ M) was shown to inhibit the activity of AMPK in neurons, upregulate the expression of p53, and then activate the mitochondrial-dependent apoptosis pathway, which may lead to neuronal apoptosis.

**Keywords:** Propofol; hippocampal; mitochondria; adenosine 5'-monophosphate (AMP)-activated protein kinase; p53

Submitted Aug 16, 2022. Accepted for publication Sep 26, 2022.

doi: 10.21037/atm-22-4374

View this article at: <https://dx.doi.org/10.21037/atm-22-4374>

<sup>A</sup> ORCID: Fei Xiao, 0000-0001-8437-8948; Yubo Xie, 0000-0002-7198-7506.

## Introduction

Our early basic research (1), and pre-clinical studies have shown neuroanatomical changes and lifetime cognitive deficits after exposure to common anesthetics at a young age (2,3). Prospective and retrospective clinical studies suggest that a single, brief exposure of a healthy individual to anesthesia will not cause long-term deficits (4,5). However, the effects of multiple or prolonged exposure to anesthesia remain unknown.

Mitochondrial functions and cellular energy levels are considered essential factors in cell survival, and modifications of these factors can trigger apoptotic cell death. Some scholars have reported that general anesthesia can cause mitochondrial dysfunction through various mechanisms, such as oxidative stress, electron transport chain dysfunction, calcium homeostasis disturbances, and mitochondria-dependent apoptosis (6,7). Propofol is a general anesthetic that is widely used anesthetic for the induction and maintenance of anesthesia and critical care sedation in children due to its rapid onset of action, rapid recovery, and no accumulation during continuous infusion. Existing research and previous studies by our group have shown that propofol can induce widespread neuroapoptosis in developing brains, which leads to cause long-term learning and memory abnormalities (1), and mitochondrial electron transport chain dysfunction, increase intracellular reactive oxygen species (ROS) production, and reduce adenosine triphosphate (ATP) levels (8), which suggests that propofol is likely to induce neurotoxicity by inhibiting mitochondrial function, which may be the reason why propofol has a toxic effect on brain development and causes long-lasting cognitive impairment (9,10).

Adenosine 5'-monophosphate (AMP)-activated protein kinase (AMPK) is a conserved energy sensor. During energy stress, AMPK directly phosphorylates key factors involved in multiple pathways to restore energy balance (11). Protein 53 (p53) is a downstream factor of AMPK, and AMPK can directly or indirectly affect the expression of p53 and then activate downstream related cell signaling pathways to induce cell apoptosis (12).

Based on the above, different concentrations or exposure times of propofol may cause varying degrees of damage to neuronal mitochondria and reduce the production of ATP. Thus, we hypothesized that a reduction in ATP could lead to the activation of AMPK. In this study, a variety of drugs were used to incubate hippocampal neurons, measure related proteins, and explore whether AMPK mediates

propofol-induced mitochondrial damage in fetal rat hippocampal neurons.

In this study we aimed to understand the potential mechanisms of the neurotoxicity of propofol and identify the role of the AMPK/p53 signaling pathway in the process. We present the following article in accordance with the ARRIVE reporting checklist (available at <https://atm.amegroups.com/article/view/10.21037/atm-22-4374/rc>).

## Methods

### *Hippocampal neuron cultures*

All the experimental procedures in this study were approved by The Animal Care and Welfare Committee of Guangxi Medical University (No. 201807290, Nanning, Guangxi, China) and implemented in accordance with the guidelines for the ethical review of laboratory animal welfare (GB/T 35892-2018). A protocol was prepared before the study without registration. Sprague-Dawley (SD) pregnant rats were provided by the experimental animal center of Guangxi Medical University. Primary hippocampal neurons were isolated from 16- to 18-day-old SD pregnant rat embryos according to previous experimental methods (13,14).

First, 1% isoflurane was used to anaesthetize the pregnant rats, and the uterus was rapidly exposed to remove the fetus, which was then anesthetized and decapitated to expose the hippocampus tissue that was then shredded under sterile conditions. The hippocampus tissue was then placed in a centrifuge tube and digested with trypsin digestion solutions (0.25%, without phenol red) (Solarbio, China, Cat#T1350) at 37 °C, for 15 minutes. When the digestive juice became turbid and the tissue became thin, the upper layer of the trypsin solution was discarded, and an equal volume of plating medium was added to terminate the digestion. At the same time, a glass pipette was used to dissociate the tissue and make them into a single-cell suspension. The single-cell suspension was seeded onto poly-lysine-coated plates (Sigma, USA, Cat#P4832) with a medium containing 88% Dulbecco's Modified Eagle Medium/Nutrient Mixture F-12 (DMEM/F12) (Gibco, USA, Cat#A4192001), 10% fetal bovine serum (Gibco, New Zealand, Cat#10091155), 1% glutamine (Sigma, USA, Cat#G7513), and 1% penicillin/streptomycin (100×, Solarbio, China, Cat#P1400) at a density of  $1-2 \times 10^6$  cells/mL in the cell incubator with 5% carbon dioxide (CO<sub>2</sub>) and 95% air at 37 °C.

After 4 hours inoculation, the medium was replaced with

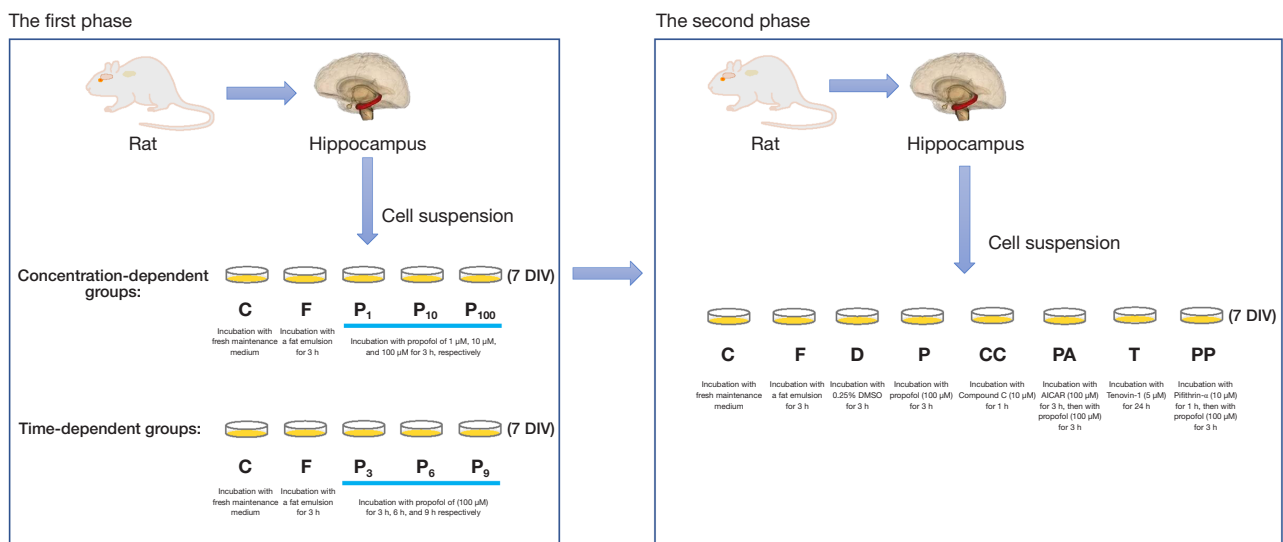


**Figure 1** Experimental groups and treatments. In the 1st phase of the study, the concentration-dependent group included hippocampal neurons that were incubated with fresh maintenance medium, a fat emulsion, and different concentrations of propofol for 3 h. In the time-dependent group, the hippocampal neurons were incubated with fresh medium, a fat emulsion and propofol (100  $\mu$ M) for 3, 6, and 9 h, respectively. In the 2nd phase of the study, the hippocampal neurons were incubated with fresh maintenance medium, a fat emulsion, 0.25% DMSO, propofol (100  $\mu$ M), compound C, AICAR, tenovin-1 and pifithrin- $\alpha$  for different times. Group C, control, fresh maintenance medium; Group F, fat emulsion; Group P<sub>1</sub>, 1  $\mu$ M propofol; Group P<sub>10</sub>, 10  $\mu$ M propofol; Group P<sub>100</sub>, 100  $\mu$ M propofol; Group P<sub>3</sub>, 100  $\mu$ M propofol for 3 h; Group P<sub>6</sub>, 100  $\mu$ M propofol for 6 h; Group P<sub>9</sub>, 100  $\mu$ M propofol for 9 h; Group D, 0.25% dimethyl sulfoxide; Group P, 100  $\mu$ M propofol for 3 h; Group CC, 10  $\mu$ M compound C for 1 h; Group PA, 100  $\mu$ M 5-aminoimidazole-4-carboxamide ribonucleotide for 3 h and 100  $\mu$ M propofol for 3 h; Group T, 5  $\mu$ M tenovin-1 for 24 h; Group PP, 10  $\mu$ M pifithrin- $\alpha$  for 1 h and 100  $\mu$ M propofol for 3 h. DMSO, dimethyl sulfoxide; AICAR, 5-Aminoimidazole-4-carboxamide-1- $\beta$ -D-ribofuranoside.

a serum-free maintenance medium that was not conducive to the growth and survival of glial cells. As a result, the final surviving cell population was mainly composed of neurons. The serum-free maintenance medium consisted of 96% neurobasal (Gibco, USA, Cat#21103049), 2% B-27 (50 $\times$ , Gibco, USA, Cat#17504044), 1% 200 mM glutamine (100 $\times$ , Sigma, USA, Cat#G7513), and 1% penicillin/streptomycin (100 $\times$ , Solarbio, China, Cat#P1400). Half of the maintenance medium was replaced every 3 days. During the culture, cell growth, morphology, density, and protuberances were observed and recorded. All of the experiments were performed after 7 days in vitro (7 DIV).

### Experimental groups and treatment

In the 1st phase of the study, petri dishes containing the 7 DIV primary hippocampal neurons were divided into 5 groups using a random-number table (see Figure 1). The concentration-dependent groups comprised Groups C, F, P<sub>1</sub>, P<sub>10</sub>, and P<sub>100</sub>. The hippocampal neurons in Groups C

and F were incubated with fresh maintenance medium and fat emulsion, respectively, for 3 h. The cells in Groups P<sub>1</sub>, P<sub>10</sub>, and P<sub>100</sub> were incubated with propofol at corresponding concentrations of 1, 10, and 100  $\mu$ M, respectively, for 3 h. The time-dependent groups comprised Groups C, F, P<sub>3</sub>, P<sub>6</sub>, and P<sub>9</sub>. The hippocampal neurons in Groups C and F were incubated with fresh medium and fat emulsion, respectively, for 3 h. The cells in Groups P<sub>3</sub>, P<sub>6</sub>, and P<sub>9</sub> were incubated with propofol (100  $\mu$ M) for 3, 6, and 9 h, respectively.

In the 2nd phase of the study, based on the experimental results of the 1st phase, the hippocampal neurons were randomly divided into Groups C, F, D, P, CC, PA, T, and PP. The cells in Groups C, F, and D were incubated with fresh medium, fat emulsion, and 0.25% dimethyl sulfoxide (DMSO), respectively, for 3 h. The cells in Group P were incubated with propofol (100  $\mu$ M) for 3 h. The cells in Group CC were incubated with the compound C (AMPK inhibitor) (10  $\mu$ M) for 1 h. The cells in Group PA were incubated with 5-aminoimidazole-4-carboxamide ribonucleotide (AICAR) (AMPK activator) (100  $\mu$ M) for

3 h and then with propofol (100  $\mu$ M) for 3 h. The cells in Group T were incubated with tenovin-1 (p53 activator) (5  $\mu$ M) for 24 h. The cells in Group PP were incubated with pifithrin- $\alpha$  (10  $\mu$ M) for 1 h and then propofol (100  $\mu$ M) for 3 h (see *Figure 1*).

Western blotting was used to measure the expression of phospho (p)-AMPK, p53, and apoptosis-related proteins, in the hippocampal neurons. We also measured the levels of ATP, ROS, and mitochondrial membrane potential. Each sample was tested at least 3 times, and each group had at least 3 independent batches of samples.

### *Western blot analysis*

After the cells in each group were incubated with the corresponding treatments, the neurons were lysed with cell lysis buffer, total protein was extracted, and the protein concentration was determined using a Bicinchoninic acid (BCA) Protein Assay Kit (Beyotime, China, Cat#P0012). Samples from each group were combined with loading buffer, and boiled for 5 minutes, separated on a 12% sodium dodecyl sulfate polyacrylamide gel electrophoresis (SDS-PAGE) gel, transferred to a polyvinylidene fluoride (PVDF) membrane (0.22  $\mu$ m, Millipore, USA) at room temperature. The membranes were blocked with skim milk for 1 h, and then incubated with antibodies against cleaved caspase-3 (1:1,000, Cell Signaling Technology, USA, Cat#9661), cleaved caspase-9 (1:1,000, Cell Signaling Technology, USA, Cat#9507), Bcl-2 (1:1,000, Abcam, USA, Cat#ab196495), Bax (1:1,000, Cell Signaling Technology, USA, Cat#2772), CytC (1:1,000, Cell Signaling Technology, USA, Cat#4272), p-AMPK (1:1,000, Cell Signaling Technology, USA, Cat#2537), p53 (1:1,000, Cell Signaling Technology, USA, Cat#9282), and GAPDH (1:5,000, Proteintech, USA, Cat#10494-1-AP) overnight at 4 °C (only cleaved caspase-9, Bcl-2, Bax, and CytC were added in the first phase of the study). Next, the membrane was washed with Tris-buffered saline/Tween 20 (TBST) (Solarbio, China, Cat#T1085) for 3 times. The membranes incubated with IRDye 680RD (1:10,000, LI-COR, Lincoln, NE) at 4 °C for 2 h. The membrane was scanned with an Odyssey membrane scanner and analyzed by Image Lab software. Glyceraldehyde-3-phosphate dehydrogenase (GAPDH) was used as the endogenous reference. The gray value of each target protein band was compared to that of the GAPDH band, and the ratio represented the expression level of each protein.

### *ATP measurement*

ATP was measured according to the method described by the manual. The medium was adsorbed, 200  $\mu$ L of lysate was added to each well of a 6-well plate, and the plate was then centrifuged at 12,000 g and 4 °C for 5 minutes and removed the supernatant. Use the diluent to dilute the ATP detection reagent at a ratio of 1:9. Next, the ATP detection solution (100  $\mu$ L) was added to the detection well at room temperature for 3–5 minutes. The sample (20  $\mu$ L) was then added to the test well and quickly mixed. After 2 sec, a photometer or liquid scintillator was used to determine the relative light unit (RLU) value or counts per minute (CPM), respectively.

### *ROS measurement*

ROS was measured according to the method described by the manual. 2,7-Dichlorodihydrofluorescein diacetate (DCFH-DA) probe fluorescence microscopy to measure the content of ROS in the primary hippocampal neurons. A serum-free medium was used to dilute the DCFH-DA (10  $\mu$ M). The medium was replaced with the DCFH-DA (10  $\mu$ M) at 37 °C for 20 minutes. The cells were washed with serum-free cell medium 3 times. The fluorescence intensity was observed under a confocal laser microscope (at an excitation wavelength of 488 nm, and an emission wavelength of 525 nm) and measured using software.

### *Mitochondrial membrane potential*

Mitochondrial membrane potential was measured according to previous experimental methods. The serum-free maintenance medium was replaced with JC-1 staining solution, mixed well, and then incubated at 37 °C for 20 minutes. During incubation, the JC-1 staining buffer (5 $\times$ ) was diluted to JC-1 staining buffer (1 $\times$ ) with distilled water at a ratio of 1:4 and placed in an ice bath. 20 minutes later, the supernatant was removed, and the cells were washed twice with the JC-1 staining buffer (1 $\times$ ). Next, an appropriate amount of cell culture medium was added into the well with hippocampal neuron, and the fluorescence microscope was used to observe the hippocampal neuron. When the membrane potential decreased, the JC-1 formed monomers and produced green fluorescence. When the membrane potential of the mitochondria was normal, the mitochondrial matrix formed a polymer and produced red fluorescence.

### Statistical analysis

All the statistical analyses were performed using SPSS statistical software package standard version 22.0 (Chicago, IL) and GraphPad Prism version 6.02 (OriginLab, USA). The data are presented as the mean  $\pm$  standard deviation (SD) for the 3 independent experiments. A 1-way analysis of variance (ANOVA) was used to analyze differences among multiple groups. A  $P < 0.05$  was considered statistically significant.

## Results

### *Propofol damaged mitochondria in hippocampal neurons in a concentration-dependent manner*

To determine whether the propofol-induced hippocampal neuron damage was related to concentration, we analyzed the apoptosis-related proteins, ATP, ROS, and mitochondrial membrane potential. The results showed that there were no significant differences in the apoptosis-related proteins, ATP, ROS, or mitochondrial membrane potential between Group C and Groups F and P<sub>1</sub> ( $P > 0.05$ ). However, ATP, mitochondrial membrane potential and Bcl-2 were significantly decreased, and ROS, Bax, CytC, and cleaved caspase-9 were significantly increased in Groups P<sub>10</sub> and P<sub>100</sub> ( $P < 0.05$ ). Compared to Group P<sub>1</sub>, ATP, mitochondrial membrane potential, and Bcl-2 were significantly decreased and ROS, Bax, CytC, and cleaved caspase-9 were significantly increased in Groups P<sub>10</sub> and P<sub>100</sub> ( $P < 0.05$ ). Compared to Group P<sub>10</sub>, ATP, mitochondrial membrane potential, and Bcl-2 were significantly decreased and ROS, Bax, CytC, and cleaved caspase-9 were significantly increased in Group P<sub>100</sub> ( $P < 0.05$ ) (see *Figure 2*).

### *Propofol damaged mitochondria in hippocampal neurons in a time-dependent manner*

To determine whether the propofol-induced damage to hippocampal neurons was related to time, we analyzed the apoptosis-related proteins, ATP, ROS, and mitochondrial membrane potential. The results showed that there were no significant differences in the apoptosis-related proteins, ATP, ROS, or mitochondrial membrane potential between Group C and Group F ( $P > 0.05$ ). However, ATP, mitochondrial membrane potential and Bcl-2 were significantly decreased, and ROS, Bax, CytC and cleaved caspase-9 were significantly increased in Groups P<sub>3</sub>, P<sub>6</sub>, and P<sub>9</sub> ( $P < 0.05$ ). Compared to Group P<sub>3</sub>, Bcl-2, ATP, and

mitochondrial membrane potential were significantly decreased, and ROS, Bax, CytC, and cleaved caspase-9 were significantly increased in Groups P<sub>6</sub> and P<sub>9</sub> ( $P < 0.05$ ). Compared to Group P<sub>6</sub>, Bcl-2, ATP, and mitochondrial membrane potential were significantly decreased, and ROS, Bax, CytC, and cleaved caspase-9 were significantly increased in Group P<sub>9</sub> ( $P < 0.05$ ) (see *Figure 3*).

### *High concentrations of propofol damaged mitochondria, inhibited AMPK activity, increased p53 expression, and activated downstream apoptosis-related pathways in neurons*

According to previous experimental results, we hypothesized that propofol (100  $\mu$ M) would seriously damage the mitochondria of the hippocampal neurons after 3 h of incubation. The results showed that compared to Group C, there was no significant difference in the relative expression of p-AMPK, p53, cleaved caspase-9, Bcl-2, Bax, cleaved caspase-3, and CytC in Groups F and D ( $P > 0.05$ ). However, p-AMPK was significantly reduced in Groups P and CC ( $P < 0.05$ ), and Bcl-2 was significantly reduced, and Bax, CytC, cleaved caspase-3, cleaved caspase-9, and p53 were significantly increased in Groups P, CC, and T ( $P < 0.05$ ). Compared to Group P, p-AMPK was significantly increased in Group PA ( $P < 0.05$ ), Bcl-2 was significantly increased, and Bax, CytC, cleaved caspase-3, cleaved caspase-9, and p53 were significantly decreased in Groups PA and PP ( $P < 0.05$ ) (see *Figure 4A-4H*).

Compared to Group C, there were no significant differences in the ATP and ROS levels or the JC-1 aggregate/JC-1 monomer ratio in Groups F and D ( $P > 0.05$ ). However, the ATP and the JC-1 aggregate/JC-1 monomer ratio were significantly reduced, and ROS was significantly increased in Groups P, CC, and T ( $P < 0.05$ ). Compared to Group P, the ATP levels and the JC-1 aggregate/JC-1 monomer ratio were significantly increased, and ROS was significantly decreased in Groups PA and PP ( $P < 0.05$ ) (see *Figures 4I-4L*).

## Discussion

The peak of neural development in the human body occurs between the 2nd trimester and the 3rd year of birth. During this period, the nervous system is vulnerable to the influence of external factors and can develop abnormally (15,16). Anesthetics commonly used in clinical practice can lead to brain damage and long-term behavioral

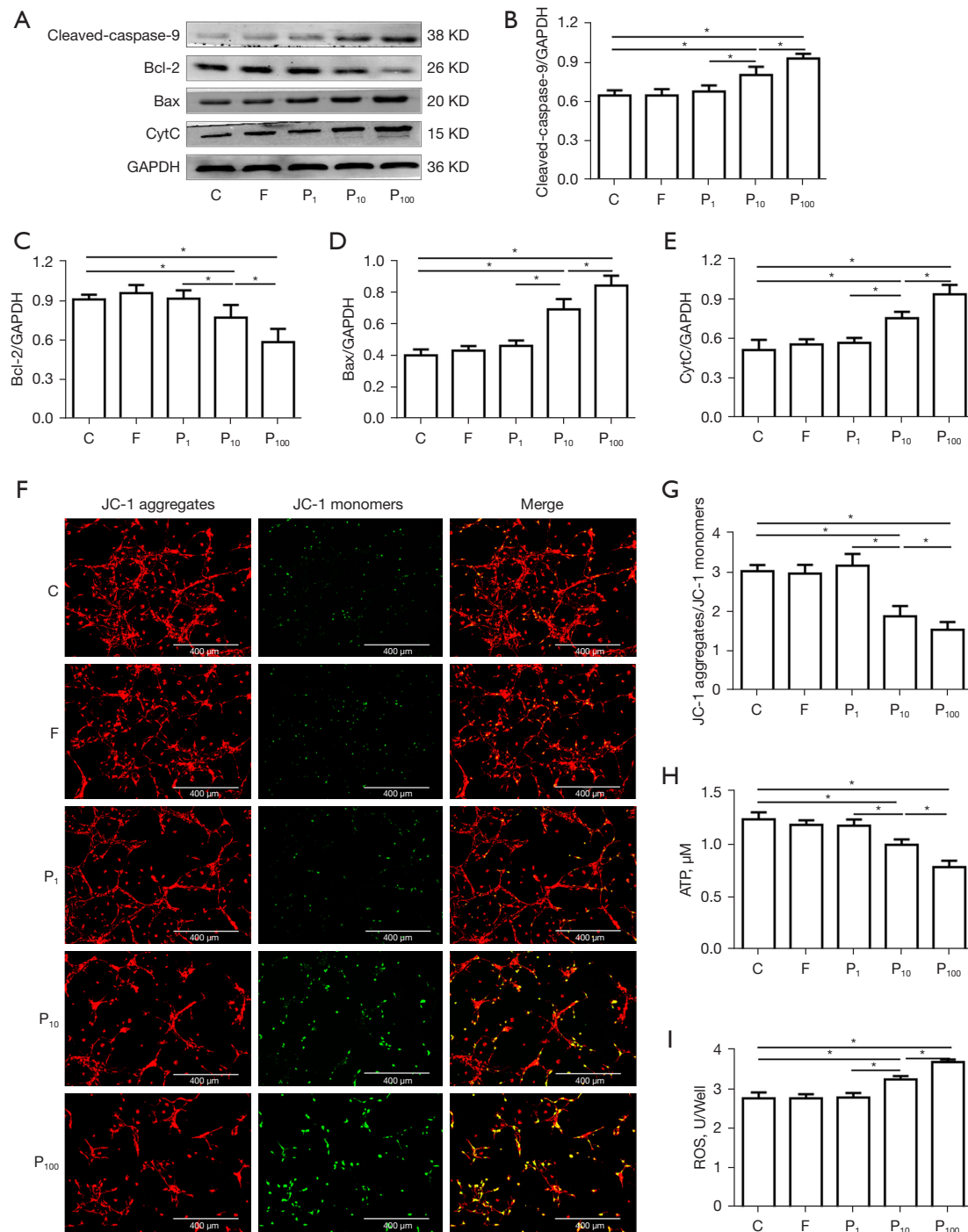


**Figure 2** Propofol damaged mitochondria in the hippocampal neurons in a concentration-dependent manner. (A) Cleaved caspase-9, Bcl-2, Bax, and CytC protein expression were detected by Western blot assay. (B-E) Quantitative analysis of the ratio of cleaved caspase-9, Bcl-2, Bax, and CytC to GAPDH (1-way ANOVA, \* $P < 0.05$ ). (F,G) Fluorescence images of JC-1 aggregates and JC-1 monomers in each group (1-way ANOVA, \* $P < 0.05$ ). (H,I) ATP and ROS content in each group (1-way ANOVA, \* $P < 0.05$ ). Group C, control, fresh maintenance medium; Group F, fat emulsion; Group P<sub>1</sub>, 1  $\mu$ M propofol; Group P<sub>10</sub>, 10  $\mu$ M propofol; Group P<sub>100</sub>, 100  $\mu$ M propofol. ANOVA, analysis of variance; ATP, adenosine triphosphate; ROS, reactive oxygen species; Bcl-2, B-cell lymphoma 2; Bax, BCL2-associated X protein; CytC, Cytochrome C; GAPDH, Glyceraldehyde-3-phosphate dehydrogenase.

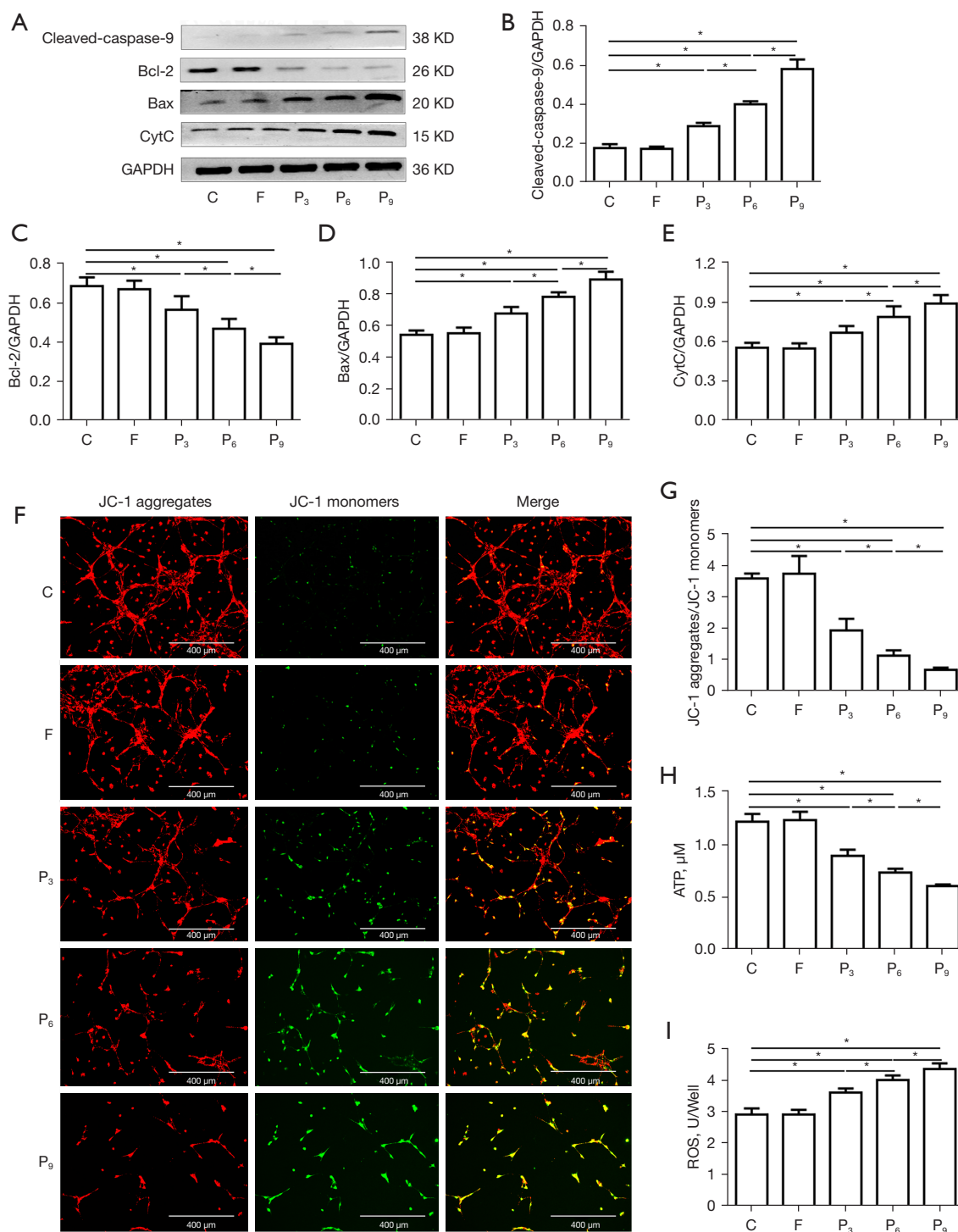


**Figure 3** Propofol damaged mitochondria in the hippocampal neurons in a time-dependent manner. (A) Cleaved caspase-9, Bcl-2, Bax, and CytC protein expression were detected by Western blot assay. (B-E) Quantitative analysis of the ratio of cleaved caspase-9, Bcl-2, Bax, and CytC to GAPDH (1-way ANOVA, \* $P < 0.05$ ). (F,G) Fluorescence images of JC-1 aggregates and JC-1 monomers in each group (1-way ANOVA, \* $P < 0.05$ ). (H,I) ATP and ROS content in each group (1-way ANOVA, \* $P < 0.05$ ). Group C, control, fresh maintenance medium; Group F, fat emulsion; Group P<sub>3</sub>, 100 μM propofol for 3 h; Group P<sub>6</sub>, 100 μM propofol for 6 h; Group P<sub>9</sub>, 100 μM propofol for 9 h. ANOVA, analysis of variance; ATP, adenosine triphosphate; ROS, reactive oxygen species; Bcl-2, B-cell lymphoma 2; Bax, BCL2-associated X protein; CytC, Cytochrome C; GAPDH, Glyceraldehyde-3-phosphate dehydrogenase.

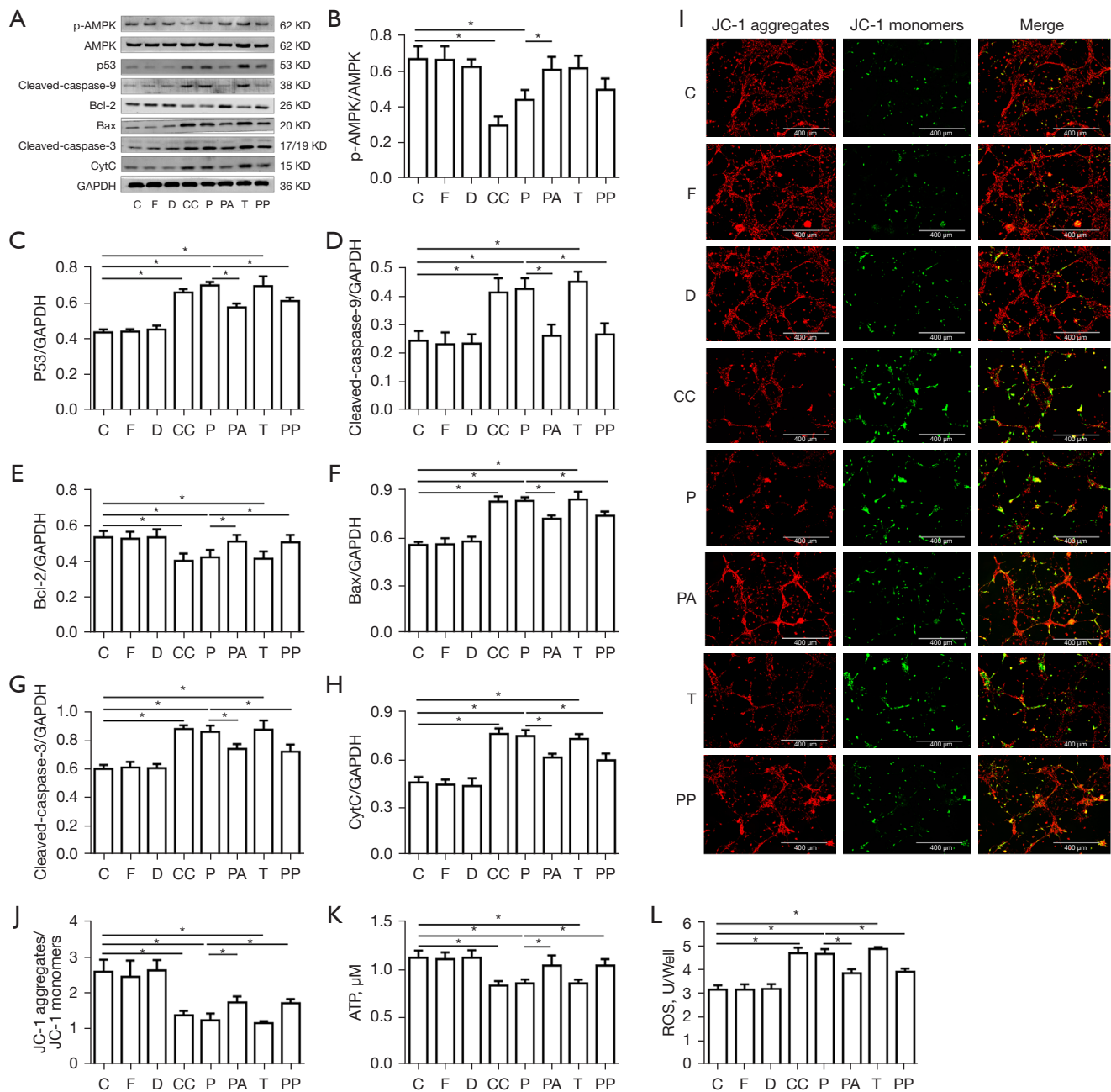


**Figure 4** High concentrations of propofol damaged the mitochondria, inhibited AMPK activity, increased p53 expression, and activated the downstream apoptosis-related pathways in neurons. (A) p-AMPK, AMPK, p53, cleaved caspase-9, Bcl-2, Bax, cleaved caspase-3, and CytC protein expression were detected by Western blot assay. (B-H) Quantitative analysis of the ratio of p-AMPK to AMPK and p53, cleaved caspase-9, Bcl-2, Bax, cleaved caspase-3, and CytC to GAPDH (1-way ANOVA, \* $P < 0.05$ ). (I-J) Fluorescence images of JC-1 aggregates and JC-1 monomers in each group (1-way ANOVA, \* $P < 0.05$ ). (K,L) ATP and ROS content in each group (1-way ANOVA, \* $P < 0.05$ ). Group C, control, fresh maintenance medium; Group F, fat emulsion; Group D, 0.25% dimethyl sulfoxide; Group P, 100  $\mu\text{M}$  propofol for 3 h; Group CC, 10  $\mu\text{M}$  compound C for 1 h; Group PA, 100  $\mu\text{M}$  5-Aminoimidazole-4-carboxamide-1-beta-D-ribofuranoside for 3 h and 100  $\mu\text{M}$  propofol for 3 h; Group T, 5  $\mu\text{M}$  tenovin-1 for 24 h; Group PP, 10  $\mu\text{M}$  pifithrin- $\alpha$  for 1 h and 100  $\mu\text{M}$  propofol for 3 h. ANOVA, analysis of variance; ATP, adenosine triphosphate; ROS, reactive oxygen species; p53, protein 53; p-AMPK, phospho-adenosine 5'-monophosphate-activated protein kinase; AMPK, adenosine 5'-monophosphate-activated protein kinase; Bcl-2, B-cell lymphoma 2; Bax, BCL2-associated X protein; CytC, Cytochrome C; GAPDH, Glyceraldehyde-3-phosphate dehydrogenase.

abnormalities during development (17). Propofol is a general anesthetic commonly used clinically in infants and young children. Existing research and previous study by our group have shown that propofol can reduce ATP production, which may be related to mitochondrial damage (18).

In the 1st phase of this study, as the concentration of propofol increased or the exposure time was prolonged, ATP levels decreased, ROS levels increased, and mitochondrial membrane potential decreased, which also suggests that propofol can cause cell mitochondrial damage. Mitochondrion-dependent apoptosis is a major apoptotic pathway. Under normal physiological conditions, anti-apoptotic proteins and proapoptotic proteins are located in the mitochondrial outer membrane and are in dynamic equilibrium. When the cells are in an abnormal state (e.g., when there is an increase in mitochondrial ROS and an attack of the mitochondrial membrane), the Bcl-2 protein family can be activated and induce cell apoptosis (19,20). Similar results were observed in our experiments. These results suggest that mitochondrial damage may be the main factor associated with propofol-induced neurotoxicity in the developing brain. Thus, the timely protection of mitochondria represents an effective strategy for inhibiting the neurotoxicity of general anesthetics.

The previous studies by our group have shown that the Erk1/2/CREB/BDNF signaling pathway (13), PKA-CREB-BDNF signaling pathway (1) and cAMP/PKA/CREB signaling pathway (19) involved in this process. Are there other signaling pathways involved in this process? In search of answers, we did the second part of the experiment. In the 2nd stage of the study, according to the FDA's recommendations for human-rat dose conversion and referring to our previous research (21), we used 100  $\mu$ M of propofol (13) as the experimental concentration for incubating neurons and analyzed the role of the AMPK and p53 in propofol-induced neuronal mitochondrial damage. AMPK is an energy-sensitive enzyme that is activated by cellular stress resulting from ATP depletion. Initially, we thought that propofol might be an inhibitor of neuronal mitochondrial energy production. After exposure to high concentrations of propofol, the ATP levels decreased and the ratio of AMP to ATP increased, which promoted AMPK phosphorylation (22). When AMPK is activated, many downstream substrate proteins, such as p53 and p27, are phosphorylated and regulate apoptosis (23). However, in this study, the AMPK activity in neurons was significantly inhibited after propofol (100  $\mu$ M) exposure, and the p53

and Bcl-2 family proteins were activated, which seems to be contradictory to the traditional mechanism by which AMPK induces apoptosis.

To further clarify the effect of AMPK in this process, we incubated neurons with compound C (AMPK inhibitor), and similar changes were observed after exposure to propofol. However, when we pre-treated the neuronal cells with AICAR (AMPK activator) and then incubated them with propofol, the above effects were reversed. Thus, propofol-induced neuronal mitochondrial damage is related to AMPK activity. It may be that the reduction in ATP does not effectively activate AMPK, and propofol plays a major role in inhibiting AMPK activity. Under different conditions, the molecular targets and effectors of AMPK-mediated cell survival are diverse, and reduced AMPK activity may induce apoptosis (24,25).

p53 is a tumor suppressor that participates in cell proliferation, differentiation, and death, and plays critical roles in both the cell cycle and apoptosis (26,27). It has been reported that p53 responds to various types of genotoxic damage and cellular stress by inducing or inhibiting the expression of >100 different genes but ultimately tends to induce apoptosis by regulating the Bcl-2 family protein pathway (28,29). In this study, we incubated the cells with a p53 activator and inhibitor, and found that compared to the control group, after exposure to propofol or tenovin-1 (the p53 activator), p53, CytC, Bax, cleaved caspase-9, and cleaved caspase-3 were upregulated, and Bcl-2 was downregulated. However, pretreatment with pifithrin- $\alpha$  (a p53 inhibitor) reversed these effects. Additionally, neither the p53 activator nor the p53 inhibitor had any significant effect on AMPK activity. Thus, p53 is the key protein for propofol-induced neuronal mitochondrial damage.

In summary, we believe that propofol-induced neuronal mitochondrial damage is mediated through the AMPK/p53 signaling pathway. The reasons are as follows: (I) Propofol activates Bcl-2 family proteins by inhibiting AMPK activity, which may induce apoptosis, and an AMPK activator can attenuate this effect; (II) the activation of Bcl-2 family proteins is mediated by p53, which can be attenuated by p53 inhibitors; and (III) P53 is the downstream substrate protein of AMPK. The activity of AMPK can affect the expression of p53. The upregulation or downregulation of p53 does not affect the activity of AMPK.

## Conclusions

Propofol (100  $\mu$ M)-induced mitochondrial damage in fetal

rat hippocampal neurons may be mediated by the AMPK/p53 signaling pathway. Propofol (100  $\mu$ M) was shown to inhibit the activity of AMPK in neurons, upregulate the expression of p53, and then activate the downstream mitochondrial-dependent apoptosis pathway, which may lead to neuronal apoptosis. Both AMPK activators and p53 inhibitors were shown to reverse the above-mentioned changes.

## Acknowledgments

**Funding:** This study was supported by Guangxi Natural Science Foundation Key Project (No. 2020GXNSFDA238025), Guangxi Key Research and Development Program (No. AB20159019), and National Key Research and Development Program (No. 2018YFC2001905).

## Footnote

**Reporting Checklist:** The authors have completed the ARRIVE reporting checklist. Available at <https://atm.amegroups.com/article/view/10.21037/atm-22-4374/rc>

**Data Sharing Statement:** Available at <https://atm.amegroups.com/article/view/10.21037/atm-22-4374/dss>

**Conflicts of Interest:** All authors have completed the ICMJE uniform disclosure form (available at <https://atm.amegroups.com/article/view/10.21037/atm-22-4374/coif>). The authors have no conflicts of interest to declare.

**Ethical Statement:** The authors are accountable for all aspects of the work in ensuring that questions related to the accuracy or integrity of any part of the work are appropriately investigated and resolved. All the experimental procedures in this study were approved by the Animal Use and Care Committee of Guangxi Medical University (No. 201807290, Nanning, Guangxi, China) and implemented in accordance with the guidelines for the ethical review of laboratory animal welfare (GB/T 35892-2018).

**Open Access Statement:** This is an Open Access article distributed in accordance with the Creative Commons Attribution-NonCommercial-NoDerivs 4.0 International License (CC BY-NC-ND 4.0), which permits the non-commercial replication and distribution of the article with the strict proviso that no changes or edits are made and the

original work is properly cited (including links to both the formal publication through the relevant DOI and the license). See: <https://creativecommons.org/licenses/by-nc-nd/4.0/>.

## References

- Zhong Y, Chen J, Li L, et al. PKA-CREB-BDNF signaling pathway mediates propofol-induced long-term learning and memory impairment in hippocampus of rats. *Brain Res* 2018;1691:64-74.
- Lin EP, Lee JR, Lee CS, et al. Do anesthetics harm the developing human brain? An integrative analysis of animal and human studies. *Neurotoxicol Teratol* 2017;60:117-28.
- Vutskits L, Xie Z. Lasting impact of general anaesthesia on the brain: mechanisms and relevance. *Nat Rev Neurosci* 2016;17:705-17.
- Wilder RT, Flick RP, Sprung J, et al. Early exposure to anesthesia and learning disabilities in a population-based birth cohort. *Anesthesiology* 2009;110:796-804.
- Sprung J, Filck RP, Katusic SK, et al. Attention-deficit/hyperactivity disorder after early exposure to procedures requiring general anesthesia. *Mayo Clin Proc* 2012;87:120-9.
- Wu J, Yang JJ, Cao Y, et al. Iron overload contributes to general anaesthesia-induced neurotoxicity and cognitive deficits. *J Neuroinflammation* 2020;17:110.
- Belrose JC, Noppens RR. Anesthesiology and cognitive impairment: a narrative review of current clinical literature. *BMC Anesthesiol* 2019;19:241.
- Herzig S, Shaw RJ. AMPK: guardian of metabolism and mitochondrial homeostasis. *Nat Rev Mol Cell Biol* 2018;19:121-35.
- Xiao F, Lv J, Liang YB, et al. The expression of glucose transporters and mitochondrial division and fusion proteins in rats exposed to hypoxic preconditioning to attenuate propofol neurotoxicity. *Int J Neurosci* 2020;130:161-9.
- Logan S, Jiang C, Yan Y, et al. Propofol Alters Long Non-Coding RNA Profiles in the Neonatal Mouse Hippocampus: Implication of Novel Mechanisms in Anesthetic-Induced Developmental Neurotoxicity. *Cell Physiol Biochem* 2018;49:2496-510.
- Garcia D, Shaw RJ. AMPK: Mechanisms of Cellular Energy Sensing and Restoration of Metabolic Balance. *Mol Cell* 2017;66:789-800.
- Chen YH, Yang SF, Yang CK, et al. Metformin induces apoptosis and inhibits migration by activating the AMPK/p53 axis and suppressing PI3K/AKT signaling in human cervical cancer cells. *Mol Med Rep* 2021;23:88.

13. Tu Y, Liang Y, Xiao Y, et al. Dexmedetomidine attenuates the neurotoxicity of propofol toward primary hippocampal neurons in vitro via Erk1/2/CREB/BDNF signaling pathways. *Drug Des Devel Ther* 2019;13:695-706.
  14. Wei Q, Chen J, Xiao F, et al. High-Dose Dexmedetomidine Promotes Apoptosis in Fetal Rat Hippocampal Neurons. *Drug Des Devel Ther* 2021;15:2433-44.
  15. Walters JL, Paule MG. Review of preclinical studies on pediatric general anesthesia-induced developmental neurotoxicity. *Neurotoxicol Teratol* 2017;60:2-23.
  16. Lv J, Liang Y, Tu Y, et al. Hypoxic preconditioning reduces propofol-induced neuroapoptosis via regulation of Bcl-2 and Bax and downregulation of activated caspase-3 in the hippocampus of neonatal rats. *Neurol Res* 2018;40:767-73.
  17. Johnson SC, Pan A, Li L, et al. Neurotoxicity of anesthetics: Mechanisms and meaning from mouse intervention studies. *Neurotoxicol Teratol* 2019;71:22-31.
  18. Yang Y, Yi J, Pan M, et al. Edaravone Alleviated Propofol-Induced Neurotoxicity in Developing Hippocampus by mBDNF/TrkB/PI3K Pathway. *Drug Des Devel Ther* 2021;15:1409-22.
  19. Guan R, Lv J, Xiao F, et al. Potential role of the cAMP/PKA/CREB signalling pathway in hypoxic preconditioning and effect on propofol-induced neurotoxicity in the hippocampus of neonatal rats. *Mol Med Rep* 2019;20:1837-45.
  20. Kale J, Osterlund EJ, Andrews DW. BCL-2 family proteins: changing partners in the dance towards death. *Cell Death Differ* 2018;25:65-80.
  21. Andropoulos DB, Greene MF. Anesthesia and Developing Brains - Implications of the FDA Warning. *N Engl J Med* 2017;376:905-7.
  22. Zhou H, Wang S, Zhu P, et al. Empagliflozin rescues diabetic myocardial microvascular injury via AMPK-mediated inhibition of mitochondrial fission. *Redox Biol* 2018;15:335-46.
  23. Deng L, Yao P, Li L, et al. p53-mediated control of aspartate-asparagine homeostasis dictates LKB1 activity and modulates cell survival. *Nat Commun* 2020;11:1755.
  24. Li MY, Zhu XL, Zhao BX, et al. Adrenomedullin alleviates the pyroptosis of Leydig cells by promoting autophagy via the ROS-AMPK-mTOR axis. *Cell Death Dis* 2019;10:489.
  25. Xin T, Lu C. SirT3 activates AMPK-related mitochondrial biogenesis and ameliorates sepsis-induced myocardial injury. *Aging (Albany NY)* 2020;12:16224-37.
  26. He YC, He L, Khoshaba R, et al. Curcumin Nicotinate Selectively Induces Cancer Cell Apoptosis and Cycle Arrest through a P53-Mediated Mechanism. *Molecules* 2019;24:4179.
  27. Mello SS, Attardi LD. Deciphering p53 signaling in tumor suppression. *Curr Opin Cell Biol* 2018;51:65-72.
  28. Mortezaee K, Salehi E, Mirtavoos-Mahyari H, et al. Mechanisms of apoptosis modulation by curcumin: Implications for cancer therapy. *J Cell Physiol* 2019;234:12537-50.
  29. Mirakhor Samani S, Ezazi Bojnordi T, Zarghampour M, et al. Expression of p53, Bcl-2 and Bax in endometrial carcinoma, endometrial hyperplasia and normal endometrium: a histopathological study. *J Obstet Gynaecol* 2018;38:999-1004.
- (English Language Editor: L. Huleatt)

**Cite this article as:** Xiao F, Qin Y, Chen J, Li C, Qin Y, Wei Y, Xie Y. The propofol-induced mitochondrial damage in fetal rat hippocampal neurons via the AMPK/P53 signaling pathway. *Ann Transl Med* 2022;10(20):1106. doi: 10.21037/atm-22-4374